

# Computer graphics applications of electron deformation densities and electrostatic potentials in coordination chemistry

Jacques Weber and Michel Roch

Laboratoire de Chimie Théorique Appliquée, Université de Genève, 30 quai Ernest Ansermet, CH-1211 Geneva 4, Switzerland

*Computer programs have been developed in order to display on a raster scan device electron deformation densities and electrostatic potentials, both as 2D colour-filled contour maps and as 3D solid models. Furthermore, as this quantum chemical model has proved to be adequate for transition metal complexes, the combined use of the  $X\alpha$  formalism and computer graphics is expected to be of value in rationalizing the reactivity of coordination and organometallic compounds. The examples of  $[\text{Cr}(\text{O}_2)_4]^{3-}$ ,  $[\text{Mo}(\text{O}_2)_4]^{2-}$  and  $[\text{Nb}(\text{O}_2)_4]^{3-}$  are discussed in an attempt to understand the differences in catalytic properties exhibited by parent metal dioxygen complexes.*

**Keywords:** quantum chemical properties, raster graphics, coordination chemistry

received 27 January 1986, accepted 3 February 1986

Molecular electrostatic potentials (MEPs) are nowadays a powerful tool for a qualitative approach to chemical reactivity<sup>1,2</sup>. Indeed, because it is a one-electron property, the electrostatic potential is easily derived from the wave-function calculated for an isolated compound and, in a first-order treatment, it may be used to describe the possible interactions of the molecule with other chemical species<sup>3,4</sup>. However, it has recently been shown that the main features of electron deformation densities (EDDs) correlate to a large extent with those of electrostatic potentials<sup>5,6</sup>, which allows the use of this property as an alternative for the study of molecular interactions. In view of the success of the MEP model for organic and bioorganic systems, it is worth using in conjunction with EDDs for inorganic and organometallic compounds, where it can be extremely useful in rationalizing and interpreting important data concerning molecular reactivities.

Whereas 2D contour maps have been used for a long time as the standard output of MEP<sup>7</sup> or EDD<sup>8</sup> calculations, 3D representations using computer graphics have been recently developed<sup>2,9-12</sup> in an attempt to provide the medicinal chemist with a convenient tool for drug design purposes. Several techniques have been used

to generate these 3D representations: they range from 3D isoenergy contours displayed as mesh or 'chicken-wire' surfaces<sup>9</sup> to colour-coded dots<sup>2,10</sup> or polygons<sup>11,12</sup> illustrating the potential value on either the van der Waals or solvent-accessible<sup>13</sup> molecular surface. There is no doubt that the revival of interest in properties such as MEPs or EDDs is primarily due to these elegant techniques of visualization, which generally allow a simultaneous manipulation of the models.

In this paper, two methods are presented which allow a convenient visualization of MEPs and EDDs on raster graphics systems: the first one uses 2D colour-filled contour maps<sup>14</sup>, i.e. 2D maps where areas between successive contours are coloured as a function of the property value; in the second one, the properties are presented as one or two isovalue coloured surfaces (corresponding to  $\pm p$ , where  $p$  is the arbitrarily chosen property value) in 3D space, obtained from solid modelling algorithms and displayed with Gouraud shading. The combined use of these two techniques of visualization of molecular properties has been found very useful for presenting the results of quantum chemical calculations to bench chemists and also for interpreting and discussing the main features of chemical bonding and reactivity in coordination compounds. As an example, the case of the tetraperoxo complexes  $[\text{Cr}(\text{O}_2)_4]^{3-}$ ,  $[\text{Mo}(\text{O}_2)_4]^{2-}$  and  $[\text{Nb}(\text{O}_2)_4]^{3-}$  will be treated here. Indeed, the particular nature of dioxygen ligands, namely the substantial differences in metal-ligand interactions they may exhibit, leads to a wide range of ionicity and nucleophilicity in this important class of compounds. This can undoubtedly be related to the unique catalytic properties of Mo(VI) dioxygen complexes for the epoxidation of alkenes<sup>6,15</sup>.

## METHODS

In an attempt to extend the range of application of these properties to inorganic and organometallic chemistry, we have recently developed techniques for calculating MEP<sup>16</sup> and EDD<sup>15</sup> maps from multiple scattering (MS)  $X\alpha$  wave-functions. When applied to small molecules, these models have been shown to lead

to properties in good agreement with those deduced from Hartree-Fock (HF) wave-functions<sup>5,15,16</sup>.

The electron density deformation  $\Delta\rho(r)$  is defined as:

$$\Delta\rho(r) = \rho_m(r) - \sum_A \rho_A(r) \quad (1)$$

where  $\rho_m(r)$  is the molecular electronic density, and  $\rho_A(r)$  is the spherically averaged electronic density of atom A, the summation running over all the atoms in the molecule.

The molecular electrostatic potential at a point  $r$  in the vicinity of a system having an electron density function  $\rho(r')$  is given by (atomic units):

$$V(r) = - \int \frac{\rho_m(r') dr'}{|r - r'|} + \sum_A \frac{Z_A}{|R_A - r|} \quad (2)$$

where  $Z_A$  is the charge on nucleus A, located at  $R_A$ . Though it is not itself an energy, the potential  $V(r)$  may be used to define isoenergy contours for the electrostatic interaction  $qV(r)$  of a proton ( $q = 1$  au) located near the molecule. We have shown that  $V(r)$  can be written in the equivalent form using the electron density deformation  $\Delta\rho(r)$ <sup>6</sup>:

$$V(r) = - \int \frac{\Delta\rho(r') dr'}{|r - r'|} + \sum_A V_A(r) \quad (3)$$

where  $V_A$  is the electrostatic potential of atom A. Practically, it is not easier to evaluate the MEP value using expression (3) rather than expression (2) since the major problems encountered in both LCAO and  $X\alpha$  formalisms remain<sup>16</sup>. However, expression (3) leads to an interesting correlation between EDD and MEP maps. Indeed, Politzer has shown that electrostatic potentials  $V_A(r)$  of free ground-state atoms are positive everywhere in the neighbourhood of the atoms<sup>17,18</sup>, which permits the conclusion that the sign of  $V(r)$  is dictated by the sign of the integral in expression (3). Negative regions of MEPs (and in particular protonation sites) should therefore be roughly located in the vicinity of the (positive) maxima of EDDs. Furthermore, preliminary results obtained for small organic molecules show that there is a good correlation between the values of EDD maxima and MEP minima<sup>19</sup>, which is another way of stating that the amount of charge transferred during bond formation is directly related to the degree of basicity of the compounds.

The molecular properties in which we are interested are derived from MS  $X\alpha$  quantum chemical calculations. They consist of numerical values calculated at each point of planar grids defined in the molecular volume. The simplest way to display the property is to draw a map of the isovalue contours. Interactive Display of Contours (IDC) is a computer program that has been developed which allows a menu driven interactive 2D display of selected contours on a colour raster screen. Two main options are available:

- standard coloured contour maps;
- coloured area maps, where areas between successive contours are coloured as a function of the property value.

In the latter case, the use of a rich palette of colours allows an immediate perception of the detailed features of the required property, such as the localization of extrema, the changes of sign, etc. The colour runs in 48 divisions from blue (positive values) to red (negative ones), the more blue (more red) the colour of the area, the higher (lower) the value of the property it represents.

In most cases, the 2D representation is adequate, but it may be interesting to represent a molecular property in real 3D space. To this end we cut the molecular volume into slices (a set of parallel planar grids) and select an isovalue contour in each slice. A triangulation algorithm, based on the connection of contours lying in successive planes, is then applied in order to generate the solid model in 3D space.

Roughly, one can say that two different kinds of algorithms are available to build a solid model from contour lines. The first one, specially used in biomedical sciences, deals with tomograms, which are successive slices close to one another, defining a continuous space and in which one can select elements of volume of same density (voxels). These voxels are then used to build the solid model<sup>21,22</sup>. The second class deals with contours defined in planes forming a discrete space: i.e. there are undefined regions of the volume between two successive planes. In this case, we no longer consider the contours as defining density areas but groups of points. Keppel<sup>23</sup> has proposed the first mathematical formulation of contour lines triangulation based on graph theory which allows the connection of two successive contours by triangles. However, this procedure is valid only if the contours in successive slices are mutually centred and are of similar size and shape. It also requires that the pairing of contours is known: i.e. a contour in one plane could be connected to  $n$  pieces of contours in another plane. If  $n \geq 2$ , Christiansen and Sederberg<sup>24</sup> provide partial solutions with a graphic editor requiring user interaction.

The MEP and EDD cases belong to the second class, but our contours are built up with 200 to 500 points and it is possible that  $n = 5$ . These algorithms are thus of no use, so we had to develop an algorithm based on geometrical grounds and leading to a simple solution in practically all cases. However, Connolly has recently suggested a triangulation procedure applied to analytical molecular surfaces for displaying solid models of the MEPs of proteins<sup>12</sup>.

## GRAPHIC SYSTEM AND PROGRAMS

Our graphic system is an AED-512B raster scan colour display with a PDP-11/60 host computer. The programs are written in FORTRAN and overlay segmented.

The IDC program uses graphical I/Os only; a menu is available and allows the user to choose all the options for the treatment of the grid of numerical values, which can not contain more than 10 000 values. Each contour is displayed in a very short time, due to a performing tracing algorithm<sup>25</sup>.

The contour lines triangulation program can handle 16 contours, each defined in different slices and with a maximum of 500 points. If a symmetry element is present in the molecule, it is possible to generate the model with part of the slices only, for example one-half in the case of a mirror plane. The output of this program is made of a file containing all the information about the triangulated solid model.

The program M3D allows then for the display of the solid model made of a mosaic of triangles, with perspective setting, hidden surfaces treatment and Gouraud shading based on a continuous tone model with one point light source<sup>26,27</sup>. Resting on a scan-line algorithm, M3D

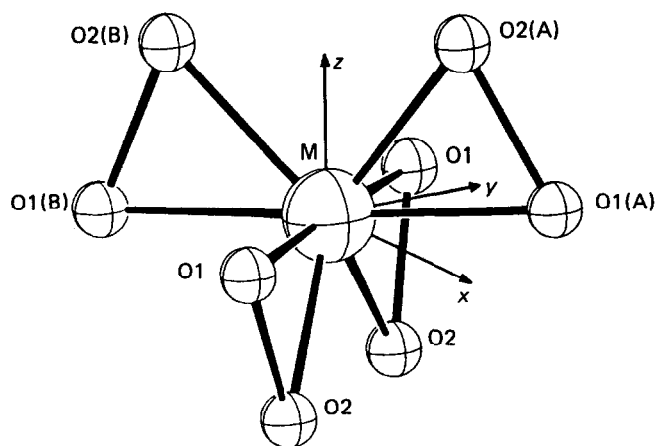


Figure 1. Structure of the  $[M(O_2)_4]^{n-}$  complex

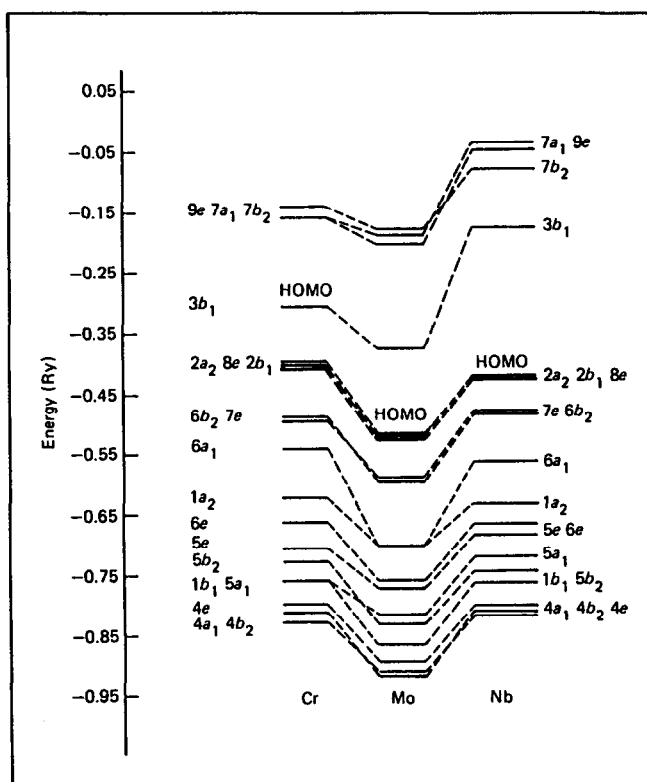


Figure 2. Upper valence ground state energy levels of the complexes. The highest occupied molecular orbitals (HOMO) are  $3b_1$  (1 electron),  $2b_1$  (2 electrons) and  $8e$  (4 electrons) for Cr, Mo, Nb complexes, respectively

allows the treatment of 500 triangles on each scan-line. The surface brightness is that of a plastic material with specular reflection of silver. Blue surfaces correspond to positive values and yellow surfaces to negative ones.

## RESULTS AND DISCUSSION

The structure of  $[Cr(O_2)_4]^{3-}$ ,  $[Mo(O_2)_4]^{2-}$  and  $[Nb(O_2)_4]^{3-}$  complexes ( $D_{2d}$  symmetry) is shown in Figure 1; all the calculation parameters have been reported elsewhere<sup>15</sup>. The electronic energy levels of the Cr(V)( $3d^1$ ), Mo(VI)( $4d^0$ ) and Nb(V)( $4d^0$ ) complexes are shown in Figure 2. Examination of this Figure indicates that the Mo complex is significantly more electrophilic than the others since its lowest unoccupied molecular orbital

(LUMO) lies about 1 eV lower than the  $3b_1$  MO of  $[Cr(O_2)_4]^{3-}$ , and about 3 eV lower than the  $3b_1$  MO of  $[Nb(O_2)_4]^{3-}$ . This conclusion will be used further to discuss the reactivity of the compounds.

Colour Plates 1(a)–1(c) show colour-filled EDD contour maps obtained for the three compounds by IDC. For the three complexes, which exhibit very similar maps except in the vicinity of the metal atom, it is seen that the formation of chemical bonds involves an important transfer from metal  $nd$  and oxygen  $2s$ ,  $2p\sigma$  electrons to O  $2p\pi$  orbitals, as revealed by the negative density peaks around metal and along the O–O bonds, and the region of charge accumulation localized on the  $\pi$ -lobes of oxygen atoms. This situation is characteristic of complexes in which metal–ligand bonding is essentially of  $\pi$  type and mainly described by a mixture of  $\pi$  orbitals of ligand with  $d$  metal orbitals.

The major difference between Colour Plates 1(a), 1(b) and 1(c) lies in the sign and shape of EDD contour maps in close vicinity of the metal atom: whereas in this region the chromium complex exhibits a large negative deformation density, the molybdenum and niobium compounds display positive lobes surrounded by small depletion regions. A detailed examination of the ground state wave-functions reveals that this different behaviour is not due to a contraction of the  $4d$  shell in Mo and Nb complexes but that it originates from differences in charge compensations between  $(n+1)p$  and  $nd$  orbitals<sup>6</sup>.

Comparison with similar EDD maps represented for the  $O_2$  molecule, the superoxide ion ( $O_2^-$ ) and the naked peroxy ligand  $O_2^{2-}$ <sup>5</sup>. (Colour Plates 2(a)–2(c)) indicate that dioxygen ligands in the complexes exhibit gross features corresponding roughly to anions  $O_2^-$ . This underlines that an important ligand to metal charge transfer occurs in the complexes. In addition, when going along the series  $O_2$ ,  $O_2^-$ ,  $O_2^{2-}$ , one notices that electron accumulation in the  $\pi$  region around the O–O bond vanishes because the  $\pi$ -bond order in these diatomics decreases from 1.0 to 0.5 and 0.0, respectively.

Colour Plates 3(a) and 3(b) illustrate 3D models of the EDD of  $O_2$  molecule displayed by M3D. The positive lobe in the  $\pi$  bonding region is clearly seen on Colour Plate 3(a) whereas in Colour Plate 3(b) it is hidden by the negative surface corresponding to electron depletion occurring at large distances.

The 2D MEPs of the complexes, Colour Plate 4, show that the protonation site is located on the O1 atom (see Figure 1) in all three cases, although this site delocalizes slightly over O2 when going from Cr to Nb. Furthermore the ordering of the MEP minima is  $Cr < Mo < Nb$ , in agreement with the order of EDD maxima of the  $\pi$ -lobes of O1 (Cr:  $0.5 \text{ e}/\text{\AA}^3$ ; Mo:  $0.6 \text{ e}/\text{\AA}^3$ ; Nb:  $1.0 \text{ e}/\text{\AA}^3$ ) which emphasizes the validity of the previously mentioned correlation between MEPs and EDDs. It should be noted that Colour Plate 4(a) could be interpreted in a misleading way after a  $90^\circ$  rotation. However, the absolute minima of the MEPs do not lie in the  $MO_2$  planes, but they are found approximately in the  $xy$  plane, in a position expected for the lobes of O1  $p\pi$  orbitals perpendicular to the plane of the Figure, as shown by Colour Plate 5. It is noteworthy that whereas the use of compensated MEPs for the negative charge of the anions allows the display of the detailed structure of the property, it is necessary to consider uncompensated MEPs when looking for the absolute minima.

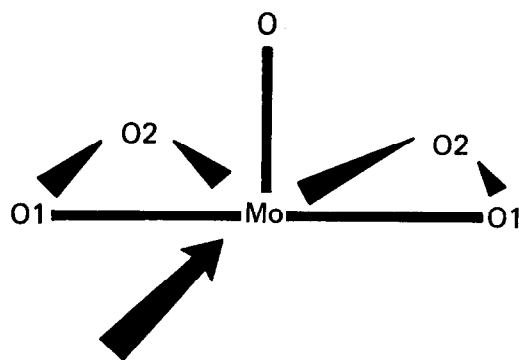


Figure 3.  $\text{MoO}(\text{O}_2)_2$  unit found in  $(\text{HMPT})\text{MoO}(\text{O}_2)_2$ . Arrow shows the favoured direction of the nucleophilic attack by the alkene

For the sake of completeness, the 2D and 3D MEPs of  $\text{O}_2$ ,  $\text{O}_2^-$  and  $\text{O}_2^{2-}$  are shown in Colour Plates 6 and 7. It is apparent that the protonation sites move significantly from nearly axial to nearly equatorial positions respectively in relation to the O–O bond. Because of the symmetry of these diatomics, the protonation sites are located at positions of cylindrical symmetry in 3D space, as shown by Colour Plate 7. Furthermore, as these MEPs are not compensated for the negative charge of the anions, they show the appearance of very large negative contours (Colour Plate 6) or surfaces (Colour Plate 7) surrounding the molecules, when going from  $\text{O}_2$  to  $\text{O}_2^{2-}$ .

Examination of Colour Plate 4 suggests that, except for  $[\text{Nb}(\text{O}_2)_4]^{3-}$ , a nucleophilic attack on the metal could occur through the blue channel located horizontally in the centre of the Figures. Furthermore, as the electronic structure of the Mo complex permits the conclusion that it has a significant electrophilic character, there is no doubt that this electrophilicity is an important factor governing the reactivity of peroxomolybdate compounds.

Unfortunately, evidence concerning the reactivity of these compounds is limited. It will be noted, however, that in the dimer  $[(\text{Ph}_3\text{P})_2\text{RhClO}_2]_2$ , where an  $\eta^2$  coordinated dioxygen ligand interacts with a second metal atom, the site of coordination of the second Rh atom corresponds to the minimum of the MEP of the compounds studied here<sup>28</sup>, which suggests that the electrostatic potential model is adequate for predicting the cation coordination sites around such clusters. Although the reactivity of the tetraperoxometallates has been little studied, the compound  $(\text{HMPT})\text{MoO}(\text{O}_2)_2$  has been shown to be an effective catalyst for the epoxidation of alkenes<sup>29</sup>. This compound contains a  $\text{Mo}(\text{O}_2)_2$  unit which may be considered as  $\text{Mo}(\text{O}_2)_4$  from which both dioxygen ligands in one plane have been removed. However, this should not modify significantly the MEP in the  $\text{Mo}(\text{O}_2)_2$  plane. Our results show that the nucleophilic attack by the incoming alkene occurs on metal and not on the nucleophilic dioxygen ligands. This is in agreement with the mechanism proposed by Mimoun<sup>29</sup>, which involves intramolecular electrophilic attack on the dioxygen by the alkene previously coordinated to the vacant site on molybdenum (see Figure 3). The present study suggests such an attack to be possible while indicating a selective electrophilic attack on the O1 atom as a second step of the reaction mechanism.

## ACKNOWLEDGEMENT

This work is part of Project 2.615–082 of the Swiss National Science Foundation. The authors would like to thank Dr A F Williams for fruitful discussions.

## REFERENCES

- 1 Scrocco, E and Tomasi, J *Advan. Quantum Chem.* Vol 11 (1978) pp 115–193
- 2 Weiner, P K et al. *Proc. Natl. Acad. Sci. USA* Vol 79 (1982) pp 3754–3758
- 3 Pullman, A and Berthod, A *Theoret. Chim. Acta* Vol 48 (1978) pp 269–277
- 4 Richards, W G *Quantum pharmacology* (2nd Edition) Butterworths, London (1983)
- 5 Roch, M and Weber, J *Chem. Phys. Lett.* Vol 115 (1985) pp 268–274
- 6 Weber, J et al. *Chem. Phys. Lett.* Vol 123 (1986) pp 246–253
- 7 Bonaccorsi, R et al. *J. Chem. Phys.* Vol 52 (1970) pp 5270–5284
- 8 Bader, R F W and Bandrauk, A D *J. Chem. Phys.* Vol 49 (1968) pp 1653–1665
- 9 Richards, W G and Sackwild, V *Chem. Britain* Vol 18 (1982) pp 635–636
- 10 Quarendon, P et al. *J. Mol. Graph.* Vol 2 (1984) pp 4–7
- 11 Nakamura, H et al. *J. Mol. Graph* Vol 2 (1984) pp 14–17
- 12 Connolly, M L *J. Appl. Cryst.* Vol 18 (1985) pp 499–505
- 13 Connolly, M L *Science* Vol 211 (1983) pp 709–713
- 14 White, D N J and Pearson, J E *J. Mol. Graph.* Vol 2 (1984) pp 60–61
- 15 Roch, M et al. *Inorg. Chem.* Vol 23 (1984) pp 4571–4580
- 16 Roch, M et al. *Chem. Phys. Lett.* Vol. 109 (1984) pp 544–549
- 17 Politzer, P in Rheingold, A L (ed) *'Homoatomic rings, chains and macromolecules of main-group elements'* Elsevier, Amsterdam (1977) pp 95–115
- 18 Weinstein, H et al. *Theoret. Chim. Acta* Vol 38 (1975) pp 159–163
- 19 Weber, J et al. *Chem. Phys. Lett.* to be submitted
- 20 Roch, M and Weber, J '3D images of molecular properties by triangulation of contour lines', to be published
- 21 Artzy, E et al. *Comput. Graph. & Image Process.* Vol 15 (1981) pp 1–25
- 22 Udupa, J K *Comput. Graph. & Image Process.* Vol 18 (1982) pp 213–235
- 23 Keppel, E *IBM J. Res. Develop.* Vol 19 (1975) pp 2–11
- 24 Christiansen, H N and Sederberg, T W *Comput. Graph.* Vol 12 (1978) pp 187–192
- 25 Roch, M *PhD thesis*, University of Geneva (1986)
- 26 Foley, J D and Van Dam, A *'Fundamentals of interactive computer graphics'* Addison-Wesley, 1982
- 27 Newmann, W M and Sproull, R F *'Principles of interactive computer graphics'* 2nd ed, McGraw-Hill, New York, 1979
- 28 Bennett, M J and Donaldson, P B *Inorg. Chem.* Vol 16 (1977) pp 1585–1589
- 29 Mimoun, H *Angew. Chem. Intern. Ed. Engl.* Vol 21 (1982) pp 734–750